Bistable Magnetic Resonance of Conduction Electrons in Solids

ARTICLE *in* THE JOURNAL OF PHYSICAL CHEMISTRY · OCTOBER 1996

Impact Factor: 2.78 · DOI: 10.1021/jp962094y

2 AUTHORS:

Laurent Binet
École nationale supérieure de chimie de Paris
86 PUBLICATIONS **1,128** CITATIONS
SEE PROFILE

Didier Gourier
French National Centre for Scientific Research
197 PUBLICATIONS **2,785** CITATIONS
SEE PROFILE

Bistable Magnetic Resonance of Conduction Electrons in Solids

Laurent Binet*,† and Didier Gourier*,†

Laboratoire de Chimie Appliquée de l'Etat Solide, Ecole Nationale Supérieure de Chimie de Paris, URA 1466 CNRS, 11 rue Pierre et Marie Curie, 75231 Paris Cedex 05, France

Received: July 15, 1996[⊗]

The phenomenon of bistable hysteresis in magnetic resonance of conduction electrons in solids is discussed, particularly the case of gallium oxide β-Ga_2O_3. This memory effect is a consequence of the dynamic polarization of nuclei by the Overhauser effect and manifests itself by a hysteresis of the ESR line provided that particular conditions for the external (or control) and internal (or material) parameters are satisfied. The influence of all these parameters on bistability is studied in detail. It is shown that magnetic resonance of conduction electrons in solids containing nonzero nuclear spins is an intrinsically bistable phenomenon. The reasons why bistability is so strong in gallium oxide even at room temperature, compared to other identified compounds where bistability exists only at very low temperature, are discussed in terms of electronic and crystallographic structure.

I. Introduction

Bistable systems have recently attracted considerable attention because of their potential use for data handling[1] or for the possible conception of neural networks.[2] This interest has been renewed lately by the discovery of the so-called stochastic resonance effect, which is described by the fact that a bistable system subjected to a small input modulated signal and to external noise has the signal-to-noise ratio of the output signal enhanced upon increasing noise intensity.[3]

Among all the possible bistable systems encountered in physics, chemistry, and biology, bistability of the interaction of an electromagnetic field with a two-level quantum system is probably the most appealing since it implies hysteresis, and thus a memory effect, in the response of an elementary entity to an external perturbation.

Free electrons moving in the conduction band of a solid and subjected to an external magnetic field constitute a simple case of independent two-level quantum systems. Following an early suggestion by Kaplan,[4] we have recently shown that the magnetic resonance of conduction electrons in solids is intrinsically bistable if several conditions are fulfilled.[5] Basically, this phenomenon is a consequence of the Overhauser effect,[6] which is the dynamic polarization of nuclear spins induced by the saturation of the magnetic resonance of conduction electrons. The additional magnetic field resulting from this nuclear polarization produces a shift of the conduction electron spin resonance (CESR) line.[7] The bistability is due to a feedback connecting the nuclear field and the saturation phenomenon which enhances the nuclear field.[8] With this bistable Overhauser effect, the CESR line exhibits a hysteresis characterized by line shapes which strongly depend on the magnetic field sweep direction. We propose to refer to this effect to as bistable conduction electron spin resonance (BCESR). This effect has been observed in β-Ga_2O_3 crystals containing conduction electrons released from oxygen vacancies.[8] It is so strong in this compound that it is easily observable even at room temperature and in moderate external field conditions (X-band, $\approx$ 0.34 T).[9]

This exceptional feature of conduction electrons in gallium oxide raises the problem of the relation between bistability and the structure of the conductor. Despite the fact that in principle the Overhauser effect is intrinsically bistable, there is no clear reason why this effect is so strong in β-Ga_2O_3. Hysteresis of CESR spectra has already been observed in some isolated cases at liquid helium temperature in metallic lithium particles,[7] in GaAs−$Al_xGa_{1-x}As$ heterostructures,[10] and in InP,[11] but these effects have not been clearly interpreted in terms of bistability of the magnetic resonance. The qualitative explanation generally given for these previous observations of hysteresis is based on the fact that the nuclear relaxation times are very long at liquid helium temperature, so that a complete nuclear polarization could be achieved only when the magnetic field is swept in the direction of displacement of the CESR line. For the other field sweep direction, the nuclear polarization is partial because the sweep time through the resonance is too short. In these cases, the hysteresis does not result from a bistable Overhauser effect. Although this explanation appears reasonable at liquid helium temperature, it is not acceptable near room temperature since the nuclear relaxation times are small and steady state nuclear polarization can be readily achieved independent of the magnetic field sweep direction.

The purpose of the present work is first to demonstrate that all the previously reported cases of hysteresis of CESR are really the manifestation of a bistable Overhauser effect. In particular, we rationalize this effect by focusing on the quantitative structure−property relation (QSPR). By QSPR we mean that in addition to the external parameters (or control parameters), all the chemical and structural parameters controlling the existence of magnetically bistable conduction electrons in solids are identified and analyzed. This should help for the identification of other materials liable to exhibit BCESR.

This paper is arranged as follows. The general features of CESR and the Overhauser effect are reviewed in section II. The basic equations describing bistability are given in section III; they can be reduced to a simple third degree equation with solutions controlled by only two independent parameters. The QSPR problem is dealt with in section IV, with analysis of the effect of all the parameters determined by the structure and the chemical nature of the compound. We show that for bistable

† E-mail: binetl@ext.jussieu.fr (L. Binet); gourierd@ext.jussieu.fr (D. Gourier).

⊗ Abstract published in *Advance ACS Abstracts,* October 1, 1996.

S0022-3654(96)02094-1 CCC: $12.00

compounds near the boundary between monostable and bistable regimes, there is a range of values for the internal (chemical and structural) parameters where bistability is extremely sensitive to small variations of these parameters.

II. General Features of ESR in Electronic Conductors

An electron in a solid subjected to an external magnetic field B_0 generally undergoes two kinds of magnetic interactions: (i) the Zeeman interaction with the external field B_0, at the origin of the ESR phenomenon, and (ii) interactions with local magnetic fields arising either from coupling with other electronic spins (spin−spin dipolar interaction) or from coupling with nonzero nuclear spins (hyperfine interaction). The static effect of these local fields, when electron spins are localized, is an inhomogeneous broadening of the ESR line width. However, in the particular case of conducting solids, these local fields are averaged by the fast motion of conduction electrons, so that the ESR line width is motionally narrowed. More precisely, the condition for motional narrowing is that the line width $\Delta\nu$ (in frequency units) in the absence of electronic motion and the correlation time τ of the motion satisfy the following criterion:[12]

$$\Delta\nu\tau \ll 1 \tag{1}$$

A. Consequences of the Motional Narrowing. The motional narrowing has two major consequences on the ESR of conduction electrons. The first one is that the spin−spin dipolar interactions are averaged to zero so that spin−spin (T_2) and spin−lattice (T_1) relaxation times are equal for an electron spin. In the case of a relaxation process resulting from interactions with phonons, Elliott's theory,[13] which assumes that these interactions are driven by spin−orbit coupling, gives an estimate of the spin relaxation time with the following expression:

$$T_1 = T_2 = a\frac{\tau}{(\Delta g)^2} \tag{2}$$

where the constant a is of the order of unity, τ is the characteristic time of conductivity, and Δg is the deviation from the free electron g value, $g_e \approx 2.0023$, which measures the magnitude of spin−orbit coupling.

The second consequence of the high mobility of conduction electrons concerns the hyperfine interaction with nonzero nuclear spins. Let us consider an electron interacting with N equivalent nuclei, each having a spin I_k, through a Fermi-type scalar interaction. The spin Hamiltonian of the electron can be written as

$$H = g\beta B_0 S_z + \sum_{k=1}^{N} A I_k S \tag{3}$$

The two terms in this equation represent, respectively, the Zeeman interaction and the hyperfine interaction. Here we have assumed the same coupling constant A for each nucleus, given by

$$A = \frac{8\pi}{3h} g\beta g_n\beta_n |\psi(0)|^2 \text{ (Hz)} \tag{4}$$

where g, β, g_n, β_n are respectively the electron g factor, the electron Bohr magneton, the nuclear g factor and the nuclear Bohr magneton. $|\psi(0)|^2$ is the electron spin density at the nucleus, which mainly arises from the contribution of s-type orbitals to the conduction band.

Let us assume that the hyperfine interaction is much smaller than the Zeeman interaction, so that only the diagonal part $AI_{z,k}S_z$ of the hyperfine interaction is conserved. With this restriction, the spin Hamiltonian becomes

$$H = g\beta B_0 S_z + \sum_{k=1}^{N} A I_{z,k} S_z \tag{5}$$

Because of the electron mobility, the electron sees only the time-average of $I_{z,k}$, which is assumed to be equal to the ensemble average $\langle I_z\rangle = (1/N)\sum_{k=1}^{N}\langle I_{z,k}\rangle$. Therefore, the Hamiltonian (5) can be reduced to a simple effective Zeeman Hamiltonian:

$$H = g\beta\left(B_0 + \frac{NA\langle I_z\rangle}{g\beta}\right)S_z \tag{6}$$

where the quantity

$$B_n = NA\langle I_z\rangle/g\beta \tag{7}$$

represents the magnetic nuclear field generated by the nuclear spin polarization $\langle I_z\rangle$. As a result, a conduction electron, delocalized over a great number of nonzero nuclear spins behaves as a free electron subjected to an effective magnetic field $B_{\text{eff}} = B_0 + B_n$. The thermal equilibrium nuclear polarization and the corresponding nuclear field are given by

$$\langle I_z\rangle = \langle I_z^0\rangle = \frac{g_n\beta_n I(I+1)B_0}{3kT} \tag{8}$$

and

$$B_n = B_n^0 = \frac{NA}{g\beta}\langle I_z^0\rangle \tag{9}$$

Since $\beta_n \ll \beta$, the thermal equilibrium value of the nuclear field B_n is in general negligibly small at high temperature compared to the external field B_0, so that the nuclear field has little effect on the CESR.

B. Dynamic Nuclear Polarization. Overhauser predicted that the nuclear field could be strongly enhanced upon saturation of the electron spin resonance.[6] The interaction between the electromagnetic field and the electron spin system is quantified by a saturation factor s, which is proportional to the CESR absorbed intensity and defined by

$$s = \frac{\langle S_z^0\rangle - \langle S_z\rangle}{\langle S_z^0\rangle} \tag{10}$$

where $\langle S_z^0\rangle$ and $\langle S_z\rangle$ are respectively the electron spin polarizations at thermal equilibrium and under microwave irradiation, the former being given by the following expression:

$$\langle S_z^0\rangle = -\frac{g\beta S(S+1)B_0}{3kT} \tag{11}$$

The saturation factor takes the value 0 at thermal equilibrium ($\langle S_z\rangle = \langle S_z^0\rangle$) and the value 1 when the populations of the electron spin states are equalized by a complete saturation ($\langle S_z\rangle = 0$). The off-diagonal part of the hyperfine Hamiltonian in eq 3, $A(I_{x,k}S_x + I_{y,k}S_y)$, induces a simultaneous relaxation of an electron spin and a nuclear spin through a "flip-flop" mechanism with the selection rule $\Delta(m_S + m_I) = 0$. Therefore, this cross relaxation deviates the nuclear spin polarization from its thermal equilibrium value when the CESR transition is

saturated. The enhanced nuclear spin polarization is then expressed by[14]

$$\langle I_z \rangle = \langle I_z^0 \rangle - sf \frac{I(I+1)}{S(S+1)} \langle S_z^0 \rangle \tag{12}$$

where the leakage factor f represents the efficiency of the nuclear polarization by the "flip-flop" relaxation process:

$$f = \frac{\nu_x}{\nu_x + \nu_n} \tag{13}$$

The nuclear relaxation rates ν_x and ν_n in eq 13 are respectively the frequency of the cross-relaxation mechanism and the nuclear relaxation frequency corresponding to all the other relaxation processes. Equation 12 shows that when the CESR transition is saturated ($s \rightarrow 1$) at strong microwave power, the nuclear spin polarization $\langle I_z \rangle$ and consequently the nuclear field B_n are greatly enhanced by approximately a factor $g\beta/g_n\beta_n \approx 10^3$ as compared with their thermal equilibrium values $\langle I_z^0 \rangle$ and B_n^0. It follows from eqs 7, 11, and 12 that for $\langle I_z \rangle \gg \langle I_z^0 \rangle$, the nuclear field B_n is related to the ESR saturation factor s by the following equation:

$$B_n = s \frac{I(I+1)NAfB_0}{3kT} = s(\Delta B_{ov})_{max} \tag{14}$$

where the quantity

$$(\Delta B_{ov})_{max} = \frac{I(I+1)NAfB_0}{3kT} \tag{15}$$

represents the highest nuclear field that can be achieved under given conditions of temperature T and external field B_0. The factor Af in eqs 14 and 15 is an ensemble average value, which in presence of several types of nuclei (several elements and isotopes) is defined by[9]

$$Af = \frac{1}{N} \sum_{k=1}^{N} p_k I_k (I_k + 1) A_k^0 |c_{s,k}|^2 f_k \tag{16}$$

In this expression p_k is the natural abundance of the nucleus k with nuclear spin I_k, A_k^0 is the hyperfine coupling constant of the kth ion (or atom) in its ^{2}S spectroscopic state, $c_{s,k}$ is the coefficient in the conduction band edge of s orbitals of the element at the kth site, and f_k is the corresponding leakage factor.

We shall now examine how the dynamic nuclear polarization, which is a general property of conducting solids with nonzero nuclear spins, may induce a bistable behavior of the conduction electron spin resonance.

III. Origin of Bistable Conduction Electron Spin Resonance (BCESR)

The basic principle of BCESR is illustrated in Figure 1. Let us consider the conduction electron spin subjected to both an external magnetic field B_0 and a saturating microwave field B_1. When the resonance condition is fulfilled, as described previously, the nuclear spins are dynamically polarized by saturation. The resulting nuclear field B_n adds to the external field B_0, which modifies in turn the resonance condition and the saturation at the origin of the nuclear polarization. Thus, the two conditions for occurrence of bistability are met: (i) a feedback loop connecting the electronic and nuclear spin systems and (ii) a nonlinear phenomenon, represented here by the saturation of the CESR transition.

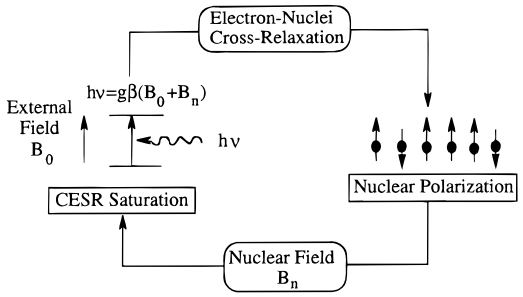

Figure 1. Feedback loop connecting the saturation and the nuclear polarization, at the origin of the bistability of the Overhauser effect.

The expression of the saturation factor s as a function of the effective static magnetic field $B_{eff} = B_0 + B_n$ experienced by the electrons, can be derived from its usual expression[12] by replacing B_0 by B_{eff}.

$$s = \frac{\gamma^2 T_1 T_2 B_1^2}{1 + \gamma^2 T_1 T_2 B_1^2 + \gamma^2 T_2^2 (B_{eff} - h\nu/g\beta)^2} \tag{17}$$

In this equation, $\gamma = g\beta/\hbar$ is the electronic gyromagnetic ratio and ν the microwave frequency. If expression 14 for the nuclear field B_n vs the saturation factor s is combined with eq 17, we obtain the two following autocoherent equations:

$$s = \frac{\gamma^2 T_1 T_2 B_1^2}{1 + \gamma^2 T_1 T_2 B_1^2 + \gamma^2 T_2^2 [B_0 + s(\Delta B_{ov})_{max} - h\nu/g\beta]^2} \tag{18}$$

$$B_n = (\Delta B_{ov})_{max} \frac{\gamma^2 T_1 T_2 B_1^2}{1 + \gamma^2 T_1 T_2 B_1^2 + \gamma^2 T_2^2 [B_0 + B_n - h\nu/g\beta]^2} \tag{19}$$

The saturation factor appears as a function of itself in eq 18 while the nuclear field is a function of itself in eq 19. These equations are strictly equivalent because of the linear relation (14) between s and B_n and correspond, respectively, to the electronic and to the nuclear aspects of bistability. Let us now define the following dimensionless parameters:

$$a = \gamma^2 T_1 T_2 B_1^2 \tag{20}$$

$$b = \gamma T_2 (\Delta B_{ov})_{max} \tag{21}$$

$$x_0 = \frac{B_0 - h\nu/g\beta}{(\Delta B_{ov})_{max}} \tag{22}$$

Equations 18 or 19 can be transformed into one single equation with the saturation factor s as the unknown:

$$s = \frac{a}{1 + a + b^2 (s + x_0)^2} \tag{23}$$

This equation is equivalent to the following third degree polynomial equation:

$$s^3 + 2x_0 s^2 + \left(\frac{1+a}{b^2} + x_0^2 \right) s - \frac{a}{b^2} = 0 \tag{24}$$

which can be further simplified by the following change of variable $s = x - 2x_0/3$, which gives a very simple form for the

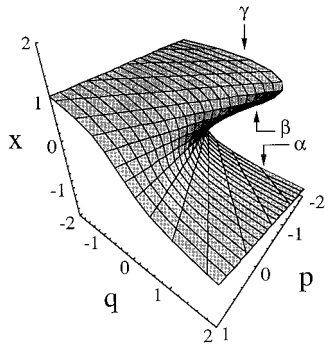

Figure 2. Solutions of eq 25, showing the monostable and the bistable regimes of the Overhauser effect.

general equation (18) of bistability:

$$x^3 + px + q = 0 \tag{25}$$

with parameters p and q defined as

$$p = \frac{1+a}{b^2} - \frac{{x_0}^2}{3} \tag{26}$$

$$q = -\frac{2{x_0}^3}{27} - \frac{2x_0(1+a)}{3b^2} - \frac{a}{b^2} \tag{27}$$

The simple form taken by eq 25 shows that despite the great number of parameters entering in eqs 18 and 19, the problem is governed only by two degrees of freedom, represented by the parameters p and q. Let us write the discriminant D of eq 25:

$$D = 4p^3 + 27q^2 \tag{28}$$

Equation 25 will exhibit one real solution if $D > 0$, two real solutions if $D = 0$, and three real solutions if $D < 0$. The variation of the solutions x vs p and q is illustrated in Figure 2. The possible existence of three real solutions, hereafter referred to as α, β and γ, implies a bistable behavior of the response x of the system when one of the parameters p or q is varied. The dimensionless parameters p and q are indeed functions of both control parameters (B_0, T, and B_1) and material parameters (T_1, T_2 and $I(I+1)NAf$). The response x of the spin system is related to the saturation factor s, that is to say the CESR absorbed intensity. This means that BCESR can be observed upon variation of any one of the control parameters and that this property can be modified by acting on the external conditions as well as on the characteristics of the material. Therefore, we can expect this form of bistability to be a general property of conducting solids with nonzero nuclear spins.

A. Hysteresis upon Variation of a Control Parameter. In this part, we suppose fixed values for the material-dependent parameters and we investigate the effect of a variation of one of the control parameters, B_0, B_1, and T, on the solutions of eqs 18 and 19. Figure 3 shows an example of the solutions of these equations as a function of the external magnetic field B_0 and actually represents the absorbed CESR intensity. Without hyperfine interaction ($(\Delta B_{ov})_{max} = 0$), the absorption curve (dotted line in Figure 3) has the usual symmetrical Lorentzian shape, meaning that the spectrum is independent on the sign of dB_0/dt. In a situation of strong enough dynamic polarization ($(\Delta B_{ov})_{max} \neq 0$), the absorption curve (full line in Figure 3) sketches out a "shark fin shape". In this case, the absorption is also proportional to the nuclear field B_n and depends on the sign of dB_0/dt. The absorbed intensity corresponds to the

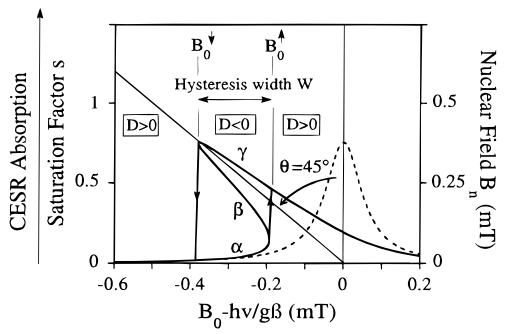

Figure 3. Calculated variations of the nuclear field B_n, the saturation factor s, and the CESR absorption vs the external magnetic field B_0 in the monostable regime (discontinuous line) and bistable regime (full line). Parameters of the calculation: $(\Delta B_{ov})_{max} = 0.5$ mT; $T_1 = T_2 = 2 \times 10^{-7}$ s; $B_1 = 5 \times 10^{-2}$ mT; $h\nu/g\beta = 342.84$ mT.

solution α of eq 18 for an increasing variation of B_0 and to the solution γ for a decreasing variation of B_0. The solution β is not obtained because it corresponds to an unstable state. The consequence is a hysteresis loop in the absorption curve, with transitions between α and γ states at different critical values $B_0^{\uparrow}$ and $B_0^{\downarrow}$ of the external field B_0 according to its direction of variation. The existence of two absorption states for a given value of the magnetic field B_0 means that the Zeeman splitting between electron spin states is different whether B_0 is increasing or decreasing. The maximum absorption occurs when the resonance condition in eqs 18 and 19 is fulfilled:

$$\frac{h\nu}{g\beta} - B_0 = B_n = s\,(\Delta B_{ov})_{max} \tag{29}$$

This means that the saturation factor and nuclear field curves vs B_0 exhibit the remarkable feature of being inclined along a line at 45° with respect to the vertical line at $B_0 - h\nu/g\beta = 0$, whatever the values of the other parameters.

This mechanism can be extended to the other control parameters, by sweeping one of them while maintaining fixed the two others. Figure 4a shows a stack plot representation of the nuclear field B_n (or the saturation factor, or the CESR absorption) vs the microwave field B_1 and the external field B_0 at fixed temperature T. Two sets of sections can be traced back across this diagram: (i) sections P_1 parallel to the (B_0, B_n) plane at fixed B_1 values, and (ii) sections P_2 parallel to the (B_1, B_n) plane at fixed B_0 values. Several sections P_1 are represented in Figure 4b, which correspond to the situation shown in Figure 3. A selected section P_2 is shown in Figure 4c. For very low values of B_1, the saturation factor and the nuclear field are single-value functions of B_0 and no hysteresis appears but when B_1 increases, s and B_n become three-value functions of B_0. The representation of s or B_n vs B_1 has an S shape. In both Figures 3 and 4, the saturation factor and the nuclear field exhibit the same variation because of the proportionality relation (eq 14) between s and B_n. A bistable behavior can be also obtained by a variation of the temperature T as shown in Figure 5. The temperature acts through the parameter $(\Delta B_{ov})_{max}$ (eq 15) but appears at nonequivalent places in eqs 18 and 19. The physical reason is that the saturation factor is always smaller than 1 while the nuclear field B_n is limited by the parameter $(\Delta B_{ov})_{max}$ which diverges when T approaches zero. Therefore, contrary to Figures 3 and 4, the curves representing the saturation factor and the nuclear field vs the temperature have different shapes (Figure 5, a and b).

B. Bistable CESR Spectra. The bistability of the microwave absorption between conduction electron spin states induces

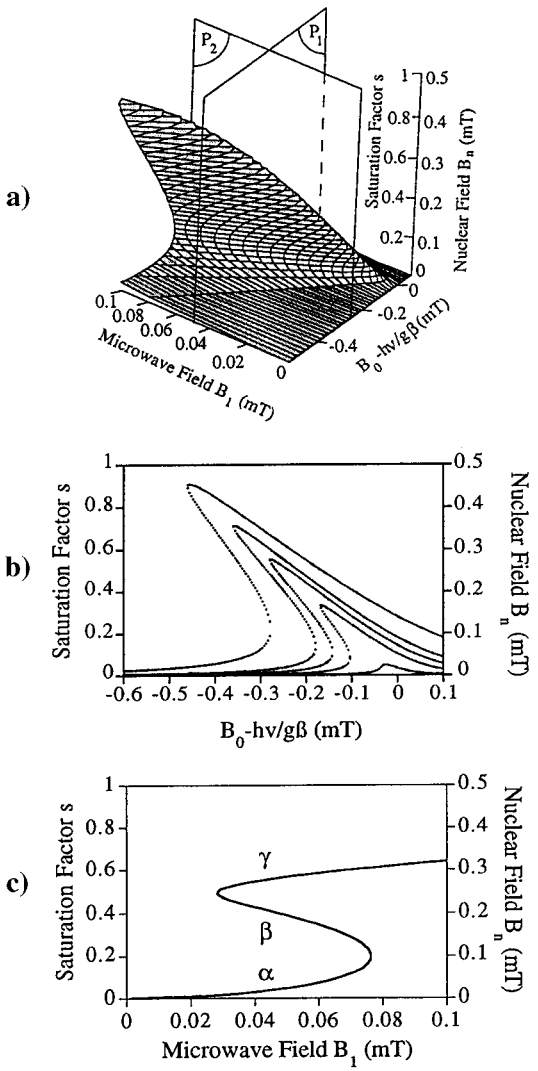

Figure 4. (a) Stack plot representation of the external field (B_0) and microwave field (B_1) dependences of the nuclear field B_n, the saturation factor s, and the CESR absorption at fixed temperature. (b) Selected sections P_1 at different values of B_1 (6×10^{-3}, 2×10^{-2}, 3.2×10^{-2}, 4.5×10^{-2}, and 8.9×10^{-2} mT). (c) Example of section P_2 at $B_0 - h\nu/g\beta = -0.25$ mT. Parameters of the calculation: $T_1 = T_2 = 2 \times 10^{-7}$ s; $(\Delta B_{ov})_{max} = 0.5$ mT.

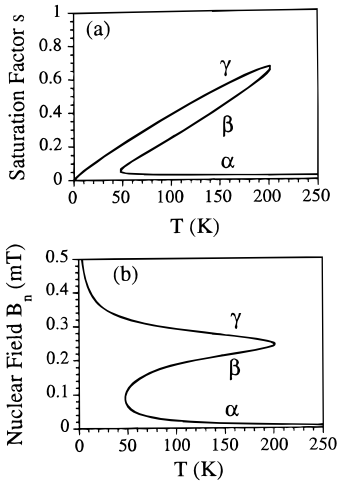

Figure 5. Temperature dependence of (a) the saturation factor s and (b) the nuclear field B_n. Parameters of the calculation: $I(I+1)NAf = 13650$ MHz; $B_0 = 345.5$ mT; $h\nu/g\beta - B_0 = 0.25$ mT; $B_1 = 4 \times 10^{-2}$ mT; $T_1 = T_2 = 2 \times 10^{-7}$ s.

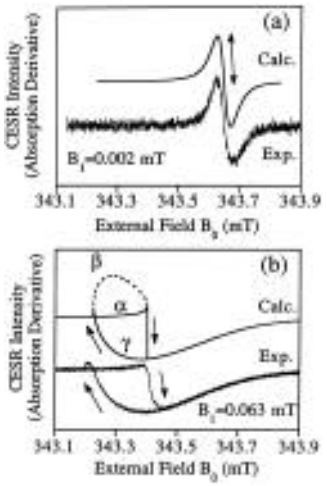

Figure 6. Examples of experimental and calculated CESR spectra for a single crystal of gallium oxide recorded at X-band ($\nu = 9432.48$ MHz) and at 150 K: (a) monostable regime; (b) bistable regime. Parameters of the calculation; $g = 1.961$; $T_1 = 1.9 \times 10^{-7}$ s; $T_2 = 1.45 \times 10^{-7}$ s; $I(I+1)NAf = 14860$ MHz.

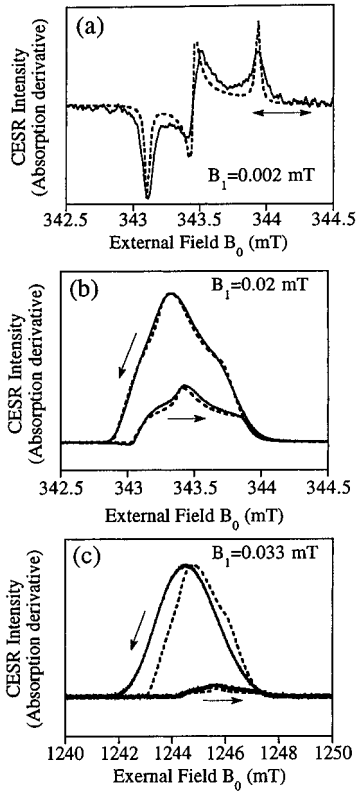

Figure 7. Examples of experimental and calculated (dotted lines) CESR spectra for a polycrystalline sample of gallium oxide. (a) Unsaturated spectrum (monostable regime) at 150 K and at X-band. (b) Saturated spectrum (bistable regime) at 150 K and at X-band. (c) Saturated spectrum (bistable regime) at 130 K and at Q-band. Parameters of the calculations: $T_1 = T_2 = 3 \times 10^{-7}$ s; $I(I+1)NAf = 13\,650$ MHz.

a hysteresis of the CESR spectra as shown in Figures 6 and 7 in the case of gallium oxide β-Ga_2O_3. These figures refer respectively, to a single crystal and to a polycrystalline sample and, for experimental reasons, represent the derivative of the CESR absorption. At low microwave field B_1, the discriminant D (eq 28) is positive whatever the value of the magnetic field B_0, and eqs 18, 19, and 25 possess only one real solution for any value of B_0. Therefore, the usual unsaturated spectrum of a $S = {}^1/_2$ spin is symmetrical and independent of the sign of dB_0/dt (Figure 6a). At high microwave field there is a domain

for B_0 characterized by $D < 0$, implying three real solutions for eqs 18, 19, and 25. So when B_0 is swept upward through this domain, solution α is observed, corresponding to the α-branch of Figure 3, with a straight transition to the γ-branch at a critical value $B_0^{\uparrow}$ of the magnetic field such that $D = 0$. When B_0 is swept downward, the solution γ is recorded, with a transition to the α-branch at another critical value $B_0^{\downarrow} < B_0^{\uparrow}$ such that $D = 0$. The result is a hysteresis of the CESR spectra (Figure 6b). The CESR intensity I_{ESR} of the experimental spectra can be simulated by the following expression:[9]

$$I_{ESR} = -I_0 \frac{B_1(B_0 + B_n - h\nu/g\beta)}{[1 + \gamma^2 T_1 T_2 B_1^{\,2} + \gamma^2 T_2^{\,2}(B_0 + B_n - h\nu/g\beta)^2]^2} \propto \frac{\partial s}{\partial B_0} \tag{30}$$

The constant I_0 depends only on temperature, instrumental parameters, and concentration of unpaired spins. The parameters T_1, T_2, and $(\Delta B_{ov})_{max}$ can be determined experimentally and therefore bistable spectra are simulated with no adjustable parameter by solving eq 19 for each value of B_0 and inserting the solutions B_n^{α} and B_n^{γ} into eq 30.

Surprisingly, the shape of bistable CESR spectra of polycrystalline samples is definitely different from that of single crystals (Figure 7). The random orientational distribution of crystallites in powder samples with respect to the external magnetic field induces a significant spectral broadening due to the *g*-tensor anisotropy. As for single crystals, at low microwave field, the CESR spectrum does not depend on the field sweep direction. It exhibits the usual powder-type shape, which in the case of β-Ga_2O_3 is characteristic of an orthorombic *g* tensor, with three singularities corresponding to the principal *g* values (Figure 7a). Bistability appears at high microwave field amplitude and manifests itself by an important difference of CESR intensities between upward and downward field sweeps (Figure 7b). Figure 7 also shows an example of the effect of the external conditions on bistability. When the applied magnetic field B_0 is increased by a factor of 4 (corresponding to Q-band), the fairly good hysteresis at X-band (Figure 7b) becomes a giant hysteresis (Figure 7c), with a strong interaction between the electron spin system and the microwave radiation in a downward field sweep but hardly any interaction in an upward field sweep. Bistable spectra can also be simulated with no adjustable parameters in the case of polycrystalline samples. The intensity of the spectrum at a given field B_0 is given by summing eq 30 over all the possible orientations of a crystallite.[15]

IV. Quantitative Structure−Property Relationship

A. Condition of Existence for BCESR. To the best of our knowledge, only a few observations of CESR lines with hysteresis have been reported so far, namely, gallium oxide,[8] metallic lithium microparticles,[7] GaAs−$Al_xGa_{1-x}As$ heterostructures,[10] and InP,[11] which could imply that this property is accidental and exists only in some isolated compounds with no apparent similarities, despite the broad generality of the theory of the bistable Overhauser effect. Moreover, in all these compounds except gallium oxide, there has been no attempt to establish a link between hysteresis and a possible bistability. Also, except for gallium oxide, this phenomenon was observed only at liquid helium temperature[7,10,11] and sometimes in high magnetic fields ($B_0 > 1$ T).[10] Gallium oxide represents an exception, for it is the unique compound exhibiting an unambiguous BCESR at room temperature and moderate magnetic field ($B_0 \approx 350$ mT).[8] It is thus evident that bistability is severely controlled by the chemical, crystallographic, and electronic structures of the compounds.

A bistable CESR spectrum will actually be observed in a conductor if the external field is swept through a range such that $D = 4p^3 + 27q^2 < 0$. This condition can only be achieved if the characteristic parameters T_1, T_2, and $I(I + 1)NAf$ of the compound and the external parameters B_0, B_1, and T satisfy a proper criterion. The discriminant D is a complicated function of these parameters and it was not possible to derive a general expression predicting a bistable resonance. However, in the case of low nuclear fields ($B_n \ll h\nu/g\beta$), the following criterion of existence for BCESR has been derived:[8]

$$\frac{I(I+1)NAf}{3kT} B_0 > \frac{8}{3\sqrt{3}} \frac{(1 + \gamma^2 T_1 T_2 B_1^{\,2})^{3/2}}{\gamma^3 T_1 T_2^{\,2} B_1^{\,2}} \tag{31}$$

This inequality represents the condition under which BCESR can be observed at a given microwave field B_1 and temperature T by sweeping B_0 over a small range about the resonance field $h\nu/g\beta$. As B_1 is a control parameter, the right-hand member of eq 31 can be minimized with respect to B_1 to give the following more general criterion of existence for BCESR:

$$b = \gamma T_2 \frac{I(I+1)NAfB_0}{3kT} > 4 \tag{32}$$

This critical inequality expresses the condition for the existence of at least one value of the microwave field B_1 for which a BCESR spectrum can be detected. The inequality first contains material-dependent parameters: the spin−spin electronic relaxation time T_2, the nuclear spin I, the hyperfine coupling constant per nucleus A, and the leakage factor f. Thus the most favorable compounds for BCESR should be characterized by long T_2, high nuclear spin, strong hyperfine interaction, and a leakage factor f close to 1. The critical inequality also contains control parameters: external magnetic field B_0 and temperature T. For a given material, the occurrence of bistability is favored by strong external magnetic field and low temperature. Therefore, the BCESR phenomenon results from a compromise between favorable material characteristics and soft external conditions, which can explain why only a few examples of this phenomenon have been observed so far. It should be stressed, however, that *the critical inequality demonstrates that bistability is a general property of conducting materials possessing nuclear spins*. The only condition is the existence of a relaxation mechanism corresponding to a simultaneous flip of electron and nuclear spins ($f \neq 0$).

Figure 8 represents two phase diagrams at 300 and 4 K with the material parameters T_2 and $I(I + 1)NAf$ taken as coordinates. The critical inequality at a fixed value of B_0 (eq 32) defines a boundary between a bistable domain (top right) and a monostable domain (bottom left). The points corresponding to various conductors are placed according to data from the literature. The relaxation time T_2 is generally determined from the unsaturated CESR line width and may be slightly underestimated if inhomogeneous broadening is present but in the case of organic conductors Fa_2AsF_6, Per_2PF_6, and Fa_2PF_6 (FA = fluoranthenyl, Per = perylenyl) direct measurements of T_2 by pulsed ESR spectroscopy were available. Values of $I(I + 1)NAf$ are provided by dynamic nuclear polarization experiments. When such data were lacking, the product NAf in eq 15 was replaced by the coupling constant A_0 of the free ion in a ^2S spectroscopic state[16] for metals and semiconductors and by the coupling

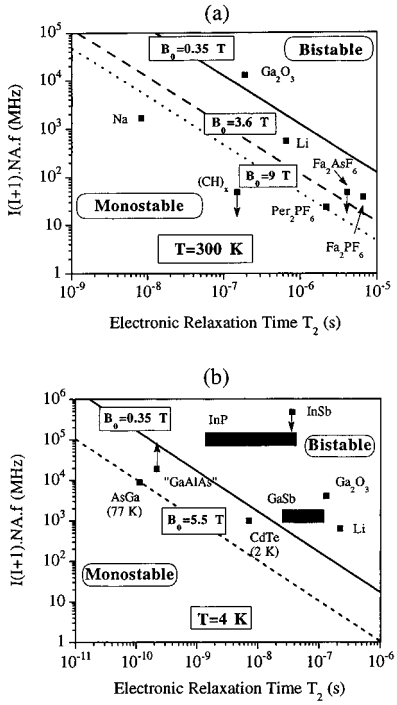

Figure 8. Phase diagram representing $I(I+1)NAf$ vs the electron spin−spin relaxation time T_2 at (a) room temperature and (b) at 4 K. The boundary between bistable regime (top) and monostable regime (bottom) at different values of the external magnetic field is represented by inclined straight lines. The theoretical positions of several conductors are indicated in the diagram.

constant $|A_\sigma| \approx 63$ MHz in the case of organic conductors for which hyperfine interaction occurs through spin polarization.[17] The value of $I(I+1)NAf$ calculated under these assumptions thus represents a theoretical upper limit and the corresponding point on the phase diagram is plotted with a downward arrow. Figure 8a shows that among conductors for which both $I(I+1)NAf$ and T_2 values are known, gallium oxide β-Ga_2O_3 is the unique conductor exhibiting bistability at room temperature and in a field of 0.35 T, for it combines both a strong hyperfine interaction and a long electron spin relaxation time. However, when the external field B_0 is increased (Figure 8a,b) or the temperature is lowered (Figure 8b), the bistability limit moves down left (discontinuous lines) allowing materials to fall into the bistable domain. Therefore, it can be predicted that organic conductors, such as Fa_2AsF_6, Per_2PF_6, and Fa_2PF_6, with the highest T_2 values known so far, should also have a bistable behavior in a high-field ESR experiment. The examples of metallic lithium particles[7] and of GaAs−$Al_xGa_{1-x}As$ heterostructures[10] and InP[11] in Figure 8b are very important for they are the only compounds along with Ga_2O_3 for which hysteresis of the conduction electron spin resonance has been observed. The diagram shows that these compounds are in the bistable domain corresponding to the conditions under which they were studied and that this hysteresis is actually due to a BCESR effect.

B. Effect of External and Material Parameters on the Hysteresis Width. In previous sections, we have investigated the conditions under which BCESR could be observed. In this section, we shall deal with the problem of the quantitative structure−property relation and discuss how this phenomenon can be influenced by both the external conditions (applied magnetic field B_0, microwave field B_1, and temperature T) and the characteristics of the material (electronic relaxation times T_1 and T_2, nuclear spin I, and effective hyperfine interaction NAf). Figures 9 and 10 illustrate the effects of the parameter $(\Delta B_{ov})_{max}$ and of the electronic relaxation times on bistability.

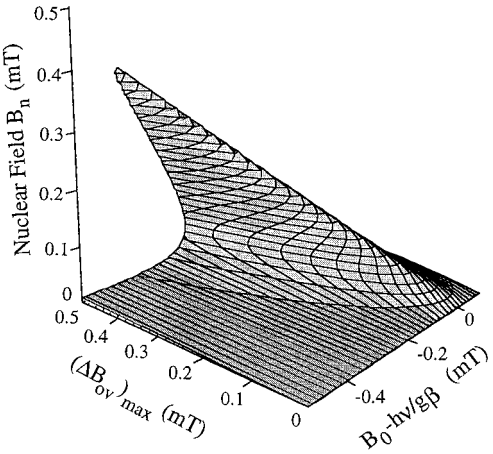

Figure 9. Influence of $(\Delta B_{ov})_{max}$ on bistability. $T_1 = T_2 = 2 \times 10^{-7}$ s; $B_1 = 6 \times 10^{-2}$ mT.

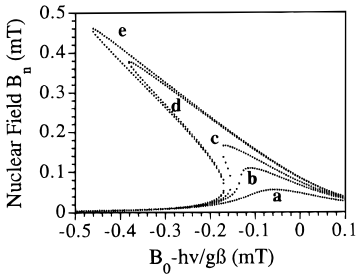

Figure 10. Influence of the electron relaxation times $T_1 \approx T_2$ on bistability. Parameters of the calculation: $I(I+1)NAf = 13650$ MHz; $T = 150$ K; $B_1 = 6 \times 10^{-2}$ mT. Values of the spin relaxation time: (a) $T_2 = 5 \times 10^{-8}$ s; (b) 7.5×10^{-8} s; (c) 10^{-7} s; (d) 2.5×10^{-7} s; and (e) 5×10^{-7} s.

It can be seen that the hysteresis increases with $(\Delta B_{ov})_{max}$ (the hollow of the map in Figure 9 grows with $(\Delta B_{ov})_{max}$) and with the relaxation times (Figure 10). In order to rationalize this behavior, let us define the hysteresis width W by

$$W = |B_0^{\uparrow} - B_0^{\downarrow}| \tag{33}$$

where $B_0^{\uparrow}$ and $B_0^{\downarrow}$ represent, respectively, the critical magnetic fields of the $\alpha \rightarrow \gamma$ and $\gamma \rightarrow \alpha$ transitions (Figure 3). These critical values correspond to the situation $D = 0$. If eq 28 is expanded using eqs 26 and 27, the following expression of the discriminant D is obtained:

$$D = {x_0}^4 + s_r {x_0}^3 + \frac{2}{b^2(1-s_r)}{x_0}^2 + \frac{9}{b^2(1-s_r)}x_0 + \frac{27{s_r}^2}{4b^2(1-s_r)} + \frac{1}{b^4(1-s_r)^2} \tag{34}$$

In this expression, we have introduced the saturation factor at resonance s_r defined by

$$s_r = \frac{a}{1+a} = \frac{\gamma^2 T_1 T_2 {B_1}^2}{1+\gamma^2 T_1 T_2 {B_1}^2} \tag{35}$$

and obtained by applying the resonance condition (29) in eq 18. The hysteresis width can then be theoretically studied using eq 34 with parameters b (see eq 21) and s_r being functions of both external and material parameters. In the following, we

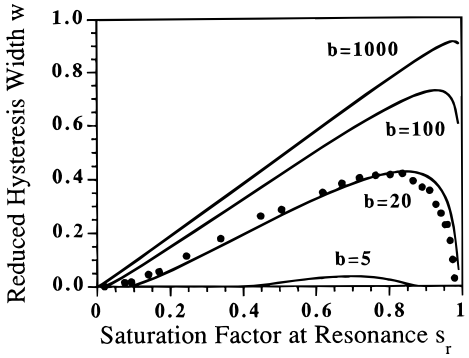

Figure 11. Variation of the reduced hysteresis width $w = W/(\Delta B_{ov})_{max}$ vs the saturation factor at resonance s_r (eq 35), for different values of the parameter b (eq 21). Circles represent the experimental points for gallium oxide at 150 K at X-band.

shall make the assumption that the nuclear field B_n is always much smaller than the applied external field B_0, which can be expressed by

$$(\Delta B_{ov})_{max} = \frac{I(I+1)NAf}{3kT} B_0 \ll h\nu/g\beta \quad (36)$$

With this condition, the CESR spectrum is obtained by sweeping B_0 over a small range about the resonance field $h\nu/g\beta$ at low saturation, and $(\Delta B_{ov})_{max}$ can be considered as constant over this range since $B_0 \approx h\nu/g\beta$. In this case the parameter x_0 varies linearly with B_0 (eq 22) and the solutions $x_0^{\uparrow}$ and $x_0^{\downarrow}$ of the polynomial equation $D(x_0) = 0$ give the hysteresis width for given values of b and s_r:

$$W = |x_0^{\uparrow} - x_0^{\downarrow}|(\Delta B_{ov})_{max} \quad (37)$$

We shall now define the reduced hysteresis width w by

$$w = \frac{W}{(\Delta B_{ov})_{max}} = |x_0^{\uparrow} - x_0^{\downarrow}| \quad (38)$$

Figure 11 shows the variation of the reduced hysteresis w vs the saturation factor at resonance s_r for different values of b, obtained by solving eq 34 numerically. For fixed values of T_1 and T_2, this picture represents the effect of B_1 upon the hysteresis width. It can be seen that the hysteresis width is nonzero only in a limited range of B_1. Inside this range, the reduced hysteresis width reaches a maximum w_{max} at a saturation factor $(s_r)_{max}$. This means that the hysteresis can be adjusted at any desired value between 0 and w_{max} by acting on the control parameter B_1. The black circles in Figure 11 correspond to experimental values of the hysteresis width measured on a single crystal of β-Ga_2O_3 at 150 K, characterized by $(\Delta B_{ov})_{max} \approx 0.45$ mT and $b \approx 20$. For high values of b (see eq 32), w tends to be linear with s_r. As a matter of fact, in this case only the first two terms dominate in eq 34. Thus, the equation $D(x_0) = 0$ has the approximate solutions $x_0^{\uparrow} \approx 0$ and $x_0^{\downarrow} \approx -s_r$, so that the reduced hysteresis width at high b value (eq 38) becomes

$$w \approx s_r \quad (39)$$

Controlling the BCESR means that one must be able to set the maximum hysteresis width W_{max} at any desired value, which limits the range of tunability. Figure 12 represents the variations of the maximum w_{max} of the reduced hysteresis width as a function of $b = \gamma T_2(\Delta B_{ov})_{max}$. This curve was calculated as follows: for a given value of b, eq 34 was numerically solved for several values of s_r between 0 and 1. The corresponding reduced hysteresis width was next calculated according to eq 38 and its maximum value w_{max} was plotted. Several remarks can be drawn from Figure 12:

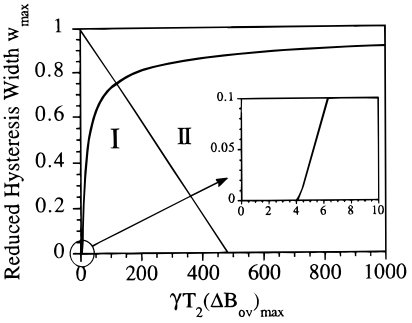

Figure 12. Theoretical variation of the maximum reduced hysteresis width w_{max} vs $\gamma T_2(\Delta B_{ov})_{max}$. Domains I and II are characterized, respectively, by a strong sensitivity and no sensitivity to small variations of internal parameters T_2 and $(\Delta B_{ov})_{max}$.

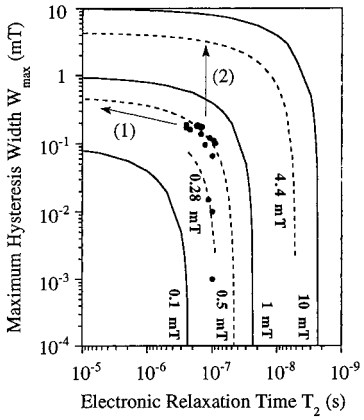

Figure 13. Variations of the maximum hysteresis width W_{max} vs the electron spin−spin relaxation time T_2 for different values of $(\Delta B_{ov})_{max}$, indicated along the corresponding curve. The values measured for 16 single crystals of gallium oxide are represented by circles.

(i) It can be seen that the maximum of the hysteresis width does not directly depend on the spin−lattice relaxation time T_1 but only on the spin−spin relaxation time T_2. This arises from the fact that T_1 is always multiplied by B_1 in eqs 18 and 19. As B_1 is a control parameter, T_1 will only determine the value of B_1 at which the maximum of the hysteresis width w_{max} will be obtained, but not the value of w_{max} itself.

(ii) Furthermore, as $\lim_{b\to 4} w_{max} = 0$, this corresponds to the threshold of existence for BCESR defined by the critical inequality (32).

(iii) When $b = \gamma T_2(\Delta B_{ov})_{max}$ is close to (but larger than) 4, which corresponds to domain I in Figure 12, w_{max} is extremely sensitive to small variations of both T_2 and $(\Delta B_{ov})_{max}$. This represents a major drawback if the sample preparation is not thoroughly controlled, because any small variation in the material characteristics will induce strong variations of the property. However, when the product $\gamma T_2(\Delta B_{ov})_{max}$ is high enough, let us say $\gamma T_2(\Delta B_{ov})_{max} \gg 4$, which corresponds to domain II in Figure 12, the reduced hysteresis width w_{max} becomes nearly constant and independent of $\gamma T_2(\Delta B_{ov})_{max}$. This means that in domain II, the absolute hysteresis width $W_{max} = w_{max}(\Delta B_{ov})_{max}$ is independent of T_2 and only linearly dependent on $(\Delta B_{ov})_{max}$.

Figure 13 shows the dispersion of the maximum hysteresis width in the case of a collection of single crystals of β-Ga_2O_3

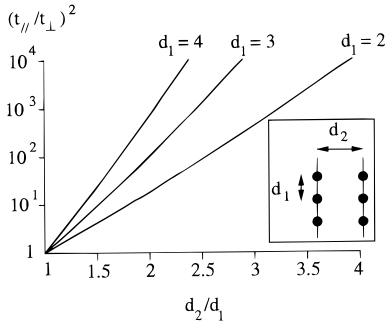

Figure 14. Simplified variation of $(t_{\parallel}/t_{\perp})^2$ vs interatomic distances, in atomic units (Bohr radius $a_0 = 0.53$ Å), in an array of one-dimensional atomic chains.

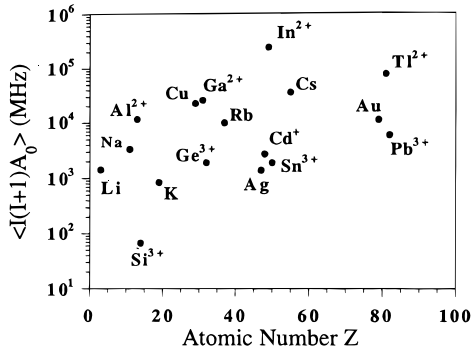

Figure 15. Theoretical values of $\langle I(I+1)A_0\rangle$ vs atomic number Z for different chemical elements in the electronic configuration s^1 (^{2}S state). The bracket indicates an average over the natural abundance of the different isotopes of the element.

synthesized according to the usual procedure.[9] These samples are divided into two groups, corresponding respectively to $(\Delta B_{ov})_{max} \approx 0.5$ mT and $(\Delta B_{ov})_{max} \approx 0.28$ mT (at 150 K). It can be noticed that these samples, and particularly the second group belong to the domain where the hysteresis width is very sensitive to any variation of T_2 and $(\Delta B_{ov})_{max}$ with hysteresis widths ranging from zero to 0.2 mT at 150 K.

C. How To Control BCESR by Material Chemistry. The conclusion from the two previous parts is that the product $\gamma T_2 (\Delta B_{ov})_{max} = b$, more explicitely defined by eq 32, is the determining parameter of BCESR since it controls at the same time the existence of bistability, its intensity, and its sensitivity to variations of external and internal parameters. It was shown that high values of b are required to have a good control of BCESR. Two strategies can be adopted to achieve such control of the phenomenon, consisting of increasing either the spin relaxation time T_2 (arrow 1 in Figure 13) or the nuclear field $(\Delta B_{ov})_{max}$ (arrow 2 in Figure 13). The nuclear field itself can be altered via two possible ways. One can first act on the external conditions, i.e., increase the applied field B_0 or decrease the temperature T since $(\Delta B_{ov})_{max}$ depends on the ratio B_0/T. On the other hand, if one needs to work under moderate field and temperature conditions, one has to act on material parameters, represented by the factor $I(I+1)NAf$.

Let us now discuss the relation between the structure of the electronic conductor and the parameters in eq 32. The first determining factor is the spin−spin relaxation time T_2, which is related to both the electronic structure of the conduction band and structural defects (impurities or intrinsic defects). The conduction band structure first determines the magnitude of the spin−orbit coupling and hence the value of Δg in eq 2. Therefore, high values of T_2 require a weak spin−orbit coupling. This can be achieved if the conduction band is built up from atomic orbitals of light elements, since the spin−orbit coupling constants λ of elements increase with their atomic number. The conduction band should also have a strong s-atomic orbital character since matrix elements of the spin−orbit Hamiltonian containing s-states vanish. However, eq 2 holds for isotropic conductors, and the anisotropy of the conduction band can also strongly influence the spin−spin relaxation times. For an anisotropic electronic structure with a preferred direction, eq 2 has to be modified in the following way:[18]

$$T_1 = T_2 = a\left(\frac{t_{\parallel}}{t_{\perp}}\right)^2 \frac{\tau}{(\Delta g)^2} \qquad (40)$$

where $t_{\parallel}$ and $t_{\perp}$ are the transfer integral, respectively, parallel and perpendicular to the preferred direction. Thus, for conductors with anisotropic band structure, with $t_{\parallel}/t_{\perp} > 1$, the spin relaxation times are greatly enhanced as compared to isotropic conductors ($t_{\parallel}/t_{\perp} = 1$). Figure 14 gives an idea of the effect of a structural anisotropy upon the band structure anisotropy (BSA) in the case of a 2D rectangular array of 1s orbitals.[19] It can be seen that the BSA measured by the ratio $(t_{\parallel}/t_{\perp})^2$, increases sharply by several orders of magnitude upon a slight variation of the ratio d_1/d_2 of the cell parameters. Therefore, the structural anisotropy must be a leading factor controlling high values of T_2. In the particular case of gallium oxide, it was stressed that the anisotropy of the conduction band, with $(t_{\parallel}/t_{\perp})^2$ of the order of 10^3-10^5 due to the particular arrangment of atoms in the material, was actually responsible for the long spin relaxation times ($T_1 \approx T_2 \approx 2 \times 10^{-7}$ s).[20] Defects can also influence the spin relaxation since collisions with structural defects or impurities can provoke spin flips. The spin−lattice relaxation time T_1 is shortened, which necessarily reduces T_2 since $T_2 \leq T_1$ in solids.

The second factor in eq 32 related to the structure of the material is the product $I(I+1)NAf$, which determines the intensity of the nuclear polarization at a given temperature and external magnetic field. In order to simplify the discussion, we shall assume that nuclei interacting with the conduction electrons belong to only one chemical element and that the leakage factor does not depend on the isotope. Thus, expression 16 for $I(I+1)NAf$ is simplified as follows:

$$I(I+1)NAf = \langle I(I+1)A_0\rangle |c_s|^2 f \qquad (41)$$

where the term in brackets is equal to

$$\langle I(I+1)A_0\rangle = \sum_k p_k I_k (I_k+1) A_k^0 \qquad (42)$$

The sum runs over all the isotopes of the element. A_0 represents the hyperfine interaction for an unpaired electron in the s-orbital of the element possessing the nuclear spin I. The factor $\langle I(I+1)A_0\rangle$ is thus determined only by the chemical element whose nuclear spins interact with conduction electrons. It can be seen that the most favorable element should have a high nuclear spin I and a strong value of the hyperfine interaction A_0, which means in general a high atomic number Z. Figure 15 gives the mean value of $I(I+1)A_0$ for several elements. It can be noticed that Cu, Ga, Cs, Tl, and mostly In are the most favorable elements for a strong nuclear polarization. Therefore, we have been endeavoring to partially substitute Ga^{3+} ions in β-Ga_2O_3 by In^{3+} so that we hope to achieve both a strong nuclear field, which can theoretically amount to 4.4 mT at room temperature thanks to indium, and a long relaxation time T_2 due to the anisotropic structure of gallium oxide.

The electronic structure also influences the intensity of the nuclear field through the contribution of s-type orbitals $|c_s|^2$ in eq 41. Therefore, conduction bands with a dominating s-

TABLE 1: Effect of Structural and Chemical Parameters on the Material Parameters T_2 and $(\Delta B_{ov})_{max}$ Controlling Bistability[a]

	electronic relaxation time T_2			maximum nuclear field $(\Delta B_{ov})_{max}$			
	$(t_{\|}/t_{\perp})$	τ	$1/(\Delta g)^2$	$I(I+1)$	A_0	$\|c_s\|^2$	f
electronic structure							
anisotropy	+						
s-character			+			+	
elements							
nuclear spin I				+			
atomic number Z			−		+		
quadrupolar moment Q							−
defects, disorder		−					−

[a] Plus and minus signs indicate which parameter (on the left) must be enhanced or reduced to increase bistability.

character due to the elements possessing the nonzero nuclear spins are required to produce strong nuclear fields. The last factor in eq 32 is the leakage factor f defined by eq 13. This factor reaches its optimal value $f = 1$ if the nuclear spins relax only via the electronic−nuclear flip-flop mechanism. So in order to avoid competing relaxation mechanisms, the material must be free of fast relaxing paramagnetic defects, and nuclei should have a low quadrupole moment to minimize the effect of quadrupolar relaxation. Table 1 summarizes the link between chemical or structural parameters on the one hand and the internal parameters controlling BCESR on the other. It is indicated which characteristic, electronic or nuclear, directly related to the chemical structure, has to be enhanced (+) or reduced (−) in order to optimize parameters T_2 and $(\Delta B_{ov})_{max}$ entering into the critical inequality (32).

V. Conclusion

The principal conclusions of this work are the following:

(i) Conduction electron spin resonance of solids containing nonzero nuclear spins is *an intrinsically bistable phenomenon*, which manifests itself by a hysteresis of the resonance line. The only condition is that nuclear spins relax (at least partially) via simultaneous flips of electron and nuclear spins in opposite directions. In that case it is always possible to find a sufficiently large value of the ratio B_0/T to allow bistability of the CESR.

(ii) In principle, it is possible to optimize this effect, i.e., to decrease the critical ratio B_0/T and to increase the hysteresis width, by acting on the chemical composition and the structure of the conducting material. The two parameters which must be enhanced to obtain an optimal effect are the maximum nuclear field $(\Delta B_{ov})_{max}$ and the electron spin−spin relaxation time T_2. In particular, chemical elements with high nuclear spin I and high Z such as indium or gallium for example, are most promising since they ensure a high value of $(\Delta B_{ov})_{max}$. On the other hand, an anisotropic band structure with a conduction band predominantly built from s-orbitals of the elements possessing the nonzero nuclear spin leads to high values of T_2. The exceptional case of gallium oxide, which exhibits bistability at room temperature, results from the fact that the high values of T_2 and $(\Delta B_{ov})_{max}$ due to is peculiar structure satisfy the critical inequality of bistability even at low B_0/T ratio.

(iii) Even if bistability conditions are satisfied, there exists a range of values of the internal parameters T_2 and $(\Delta B_{ov})_{max}$ for which bistability is extremely sensitive to any small variation of either of these two parameters. This situation occurs when T_2 and $(\Delta B_{ov})_{max}$ are just above their threshold value for bistability. The latter becomes stable against small variation of materials parameters only if these are far from their threshold values.

References and Notes

(1) Gibbs, H. M.; Mandel, P.; Peyghambarian, N.; Smith, S. D. *Optical bistability*; Springer: Berlin, 1986.
(2) Linder, J. F.; Meadows, B. K.; Ditto, W. L.; Inchiosa, M. E.; Bulsara, A. R. *Phys. Rev. Lett.* **1995**, *75*, 3 and references therein.
(3) Weisenfeld, K.; Moss, F. *Nature* **1995**, *373*, 33 and references therein.
(4) Kaplan, J. I. *Phys. Rev.* **1955**, *99*, 1322.
(5) Aubay, E.; Gourier, D. *Solid State Commun.* **1993**, *85*, 821.
(6) Overhauser, A. *Phys. Rev.* **1953**, *92*, 411.
(7) Gueron, M.; Ryter, C. *Phys. Rev. Lett.* **1959**, *3*, 338.
(8) Aubay, E.; Gourier, D. *J. Phys. Chem.* **1992**, *96*, 5513.
(9) Aubay, E.; Gourier, D. *Phys. Rev. B* **1993**, *47*, 15023.
(10) Dobers, M.; v.Klitzing, K.; Schneider, J.; Weimann, G.; Ploog, K. *Phys. Rev. Lett.* **1988**, *61*, 1650.
(11) Binet, L.; Gourier, D. To be published.
(12) Abragam, A. *Principles of Nuclear Magnetism*; Clarendon; Oxford, U.K., 1983.
(13) Elliott, R. J. *Phys. Rev.* **1954**, *96*, 266.
(14) Solomon, I. *Phys. Rev.* **1955**, *99*, 559.
(15) Gourier, D.; Binet, L.; Aubay, E. *J. Chim. Phys. (Fr.)* **1995**, *92*, 1831.
(16) Gordy, W. *Theory and Application of Electron Spin Resonance*; Wiley: New York, 1980.
(17) Mc Connell, H. M.; Chesnut, D. B. *J. Chem. Phys.* **1958**, *28*, 107.
(18) Tomkiewicz, Y.; Taranko, A. R. *Phys. Rev. B* **1978**, *18*, 733.
(19) $t_{\|}$ and $t_{\perp}$ are related to the energy splitting $W(d)$ between bonding and antibonding states of H_2^+ by $(t_{\|}/t_{\perp})^2 = [W(d_1)/W(d_2)]^2$, with $W(d) = 2(K - SJ)/(1 - S^2)$. The parameters J, K, and S represent, respectively, the Coulombic integral, the exchange integral, and the overlap integral. These are given by $S = e^{-d}(d^2/3 + d + 1)$, $J = 2e^{-2d}(1 + 1/d) - 2/d$ and $K = -2e^{-d}(d + 1)$.
(20) Binet, L.; Gourier, D.; Minot, C. *J. Solid State Chem.* **1994**, *113*, 420.

JP962094Y